

High-Efficiency Multiplexed Cytosine Base Editors for Natural Product Synthesis in *Yarrowia lipolytica*

Vijaydev Ganesan, Lummy Monteiro, Dheeraj Pedada, Anthony Stohr, and Mark Blenner*

Cite This: *ACS Synth. Biol.* 2023, 12, 3082–3091

Read Online

ACCESS |



Metrics & More



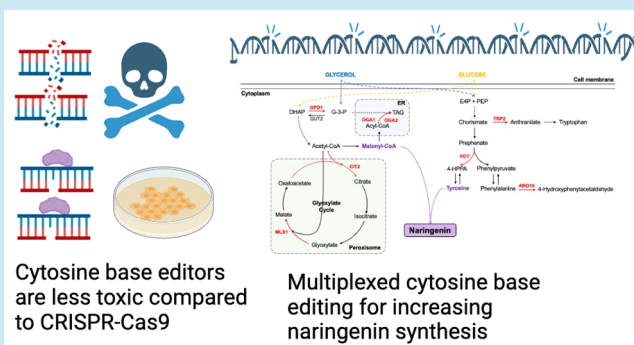
Article Recommendations



Supporting Information

ABSTRACT: *Yarrowia lipolytica* is an industrial host with a high fatty acid flux. Even though CRISPR-based tools have accelerated its metabolic engineering, there remains a need to develop tools for rapid multiplexed strain engineering to accelerate the design–build–test–learn cycle. Base editors have the potential to perform high-efficiency multiplexed gene editing because they do not depend upon double-stranded DNA breaks. Here, we identified that base editors are less toxic than CRISPR-Cas9 for multiplexed gene editing. We increased the editing efficiency by removing the extra nucleotides between tRNA and gRNA and increasing the base editor and gRNA copy number in a Ku70 deficient strain. We achieved five multiplexed gene editing in the Δ Ku70 strain at 42% efficiency. Initially, we were unsuccessful at performing multiplexed base editing in NHEJ competent strain; however, we increased the editing efficiency by using a co-selection approach to enrich base editing events. Base editor-mediated canavanine gene (CAN1) knockout provided resistance to the import of canavanine, which enriched the base editing in other unrelated genetic loci. We performed multiplexed editing of up to three genes at 40% efficiency in the Po1f strain through the CAN1 co-selection approach. Finally, we demonstrated the application of multiplexed cytosine base editor for rapid multigene knockout to increase naringenin production by 2-fold from glucose or glycerol as a carbon source.

KEYWORDS: CRISPR-Cas9, nonconventional yeast, metabolic engineering, multiplexed gene editing, cytosine base editor, Golden Gate



1. INTRODUCTION

Yarrowia lipolytica is an oleaginous industrial host used to produce lipid-based products due to its high fatty acid flux and the ability to use alternative substrates such as crude glycerol,¹ xylose,² and urine.³ It has been engineered to produce 99 g/L lipids and up to 90% dry cell weight.⁴ Specific fatty acids and fatty acid-derived products (e.g., omega-3 fatty acids⁵ and fatty alcohols^{6,7}) have been engineered. The intrinsic properties of oleaginous yeast have also been leveraged for the production of small molecules such as flavonoids^{8,9} and carotenoids^{10,11} that draw their precursors from the same high flux intermediates. Much of the recent advances in processes using *Y. lipolytica* are enabled by rapid progress creating genetic tools, such as tunable promoters,^{12,13} inducible promoters,^{14–16} Golden Gate assembly kits,^{17–20} and a variety of CRISPR-Cas9 systems.^{21–23}

Even though CRISPR-based tools have accelerated metabolic engineering in *Y. lipolytica*, genome engineering has proven difficult compared to *Saccharomyces cerevisiae* due to the activity of nonhomologous end joining (NHEJ) in *Y. lipolytica* compared to homology-directed repair (HDR). Single gene deletion was previously done in *Y. lipolytica* with CRISPR-Cas9 or Cpf1 using sgRNAs controlled by Pol III promoters.^{21–25} However, metabolic engineering requires

multiple perturbations to increase the production of a target molecule. Previously, Cpf1-based multiplexed gene editing was done in *Y. lipolytica* Po1f strain using AsCpf1²⁶ and LbCpf1.²⁷ The multiplexed editing efficiency was 41.7% for AsCpf1 and 44% for LbCpf1 for the three-gene targets. However, multiplexed editing was not accomplished in the Ku70 deficient strain. Knocking out the Ku70 gene biases the cell's DNA repair machinery to induce HDR, making it easier to integrate heterologous DNA. Po1f strain is the wild-type strain without any bias toward HDR repair and performs NHEJ to repair DNA breaks. It is important to develop tools for both strains to accelerate strain engineering. Multiplexed editing was limited to three edits due to the potential toxicity from double-stranded DNA breaks, as both Cpf1s rely on double-stranded DNA breaks. An alternative platform must be considered to accelerate multiplexed gene editing in *Y. lipolytica*. When CRISPR-Cas9 was used to knock out multiple genes in the

Received: July 20, 2023

Published: September 28, 2023



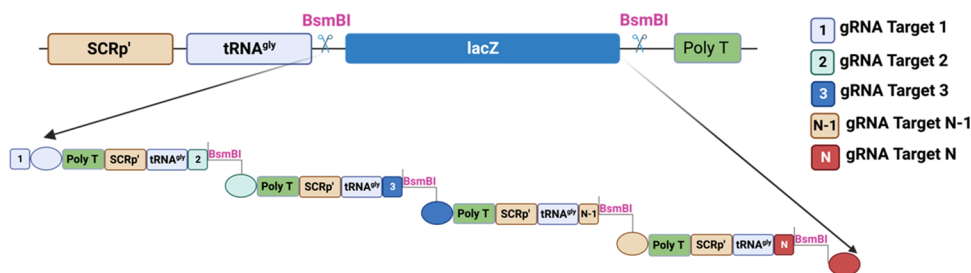


Figure 1. One-step Golden Gate-based assembly for multiplexed monocistronic gRNAs without pre-cloning. Multiplexed monocistronic gRNA plasmid is constructed by Golden Gate assembly of PCR fragments containing a gRNA array and replacing lacZ reporter with gRNA cassettes. N denotes the number of gRNAs that can be assembled using the Golden Gate design.

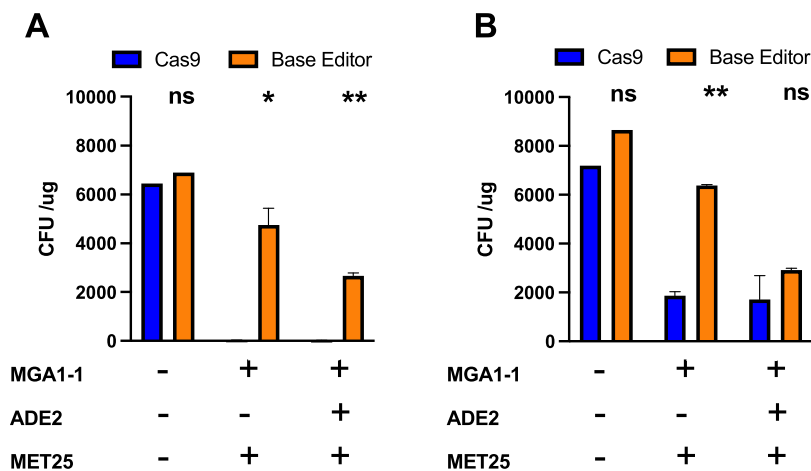


Figure 2. Nickase base editor results in higher transformation efficiency than Cas9. (A) Transformation efficiency in Δ Ku70 strain. (B) Transformation efficiency in Po1f strain. Data is based on colony counts from two independent transformations obtained by transforming equal amounts of DNA. The colony count was baselined to the control DNA. The control was an expression of the base editor or Cas9 without any gRNA target. Statistical significance was evaluated using the Student's two-tailed *t* test. Error bars represent the standard error calculated between two biological replicates. Single asterisk indicates a *p*-value of 0.06–0.10, double asterisk indicates a *p*-value < 0.05, and ns indicates *p*-value > 0.10.

POX family, chromosomal rearrangements were caused, thus showing the limitation of CRISPR-Cas9-based DSB for multiplexed knockouts.²⁸

Cytosine base editors are an alternative to CRISPR-Cas9 for gene editing without creating double-stranded DNA breaks, thus alleviating potential toxicity and chromosomal rearrangements. Cytosine base editors deaminate cytosine to uracil, which is further converted to thymine due to the base excision repair pathway. Previously, a cytosine base editor was developed in *Y. lipolytica* to perform multiplexed base editing up to two targets.²⁹ Nicking the complementary strand using nCas9(D10A) resulted in a higher editing efficiency than binding using dead Cas9(D10A H840A). Multiplexed knock-out efficiency was 31% for PEX10 and TRP1. However, the base editing was observed only for strain carrying the NHEJ-deficient Ku70 knockout and not for the wild-type Po1f strain. 50% of the right clones had indels in the Po1f strain.

Here, we increased the base editing efficiency by removing extra nucleotides between tRNA and gRNA, similar to the data observed for CRISPR-Cas9-based knockouts.³⁰ We increased the multiplexed base editing efficiency to 83% for three-gene targets using the optimized gRNA design. We extended it to 5-gene editing with an efficiency of 16%. We increased multiplexed base editing efficiency to 42% on 5-gene targets in the Δ Ku70 strain by increasing the copy number of gRNA and Base editor. We addressed the poor editing efficiency in the Po1f strain by using a CAN1-based co-selection approach.

We performed multiplexed base editing up to three targets with 40% editing efficiency in Po1f strain using the CAN1-based co-selection system, which is on par with the current multiplexed editing ability of Cpf1. Finally, to demonstrate the application of multiplexed base editing, we increased the production of the natural product naringenin with different carbon sources by performing multiplexed knockouts to increase malonyl-CoA and tyrosine flux. We split the naringenin metabolic pathway into tyrosine and the malonyl-CoA module and probed each module by performing multiplexed knockouts. We observed a 2-fold increase in naringenin production with base editor-based knockouts compared to the wild-type strain with glycerol and glucose as the carbon source, thus demonstrating the application of cytosine base editor to accelerate strain development for metabolic engineering applications. We also identified that naringenin synthesis can be increased by knocking out genes in the glyoxylate cycle to increase the acetyl-CoA flux or by knocking out genes in the aromatic amino acid biosynthesis metabolic pathway to increase the tyrosine flux.

2. RESULTS AND DISCUSSION

2.1. Golden Gate System for Efficient Multiplexed Assembly of gRNA Cassettes.

Multiple gRNAs are needed for targeting multiple genes to perform multiplexed editing. Multiple gRNAs could be expressed by using plasmids containing multiple selection markers. However, this requires

the extended curing of plasmids. Gibson assembly could be used to assemble various gRNAs. For example, Gibson assembly was used to assemble various gRNAs for multiplexed gene editing using dCas9-based CRISPRa,³³ CRISPRi,³⁴ and Cpf1.²⁷ However, repeats and multiple clonings make it inconsistent, laborious, and difficult to scale. A custom Golden Gate system was designed with the type II enzyme, BsmBI, to assemble multiple gRNAs without pre-cloning (Figure 1). LacZ was used as a reporter to monitor the cloning efficiency. This Golden Gate system was tested to assemble up to five gRNA cassettes at >30% assembly efficiency and three targets at >70% assembly efficiency (data not shown). The system could also be used for multiplexed assembly for any CRISPR-Cas9-based system, including the recently developed dCas9-based CRISPRa³³ and CRISPRi.³⁴

2.2. Toxicity of Double-Stranded Breaks Limits Multiplexed Gene Editing. We compared the toxicity of Cas9-based dsDNA breaks with nCas9(D10A) based cytosine base editors using gRNAs that targeted nonessential genes MGA1, ADE2, and MET25 in double and triple multiplexed editing (Figure 2). MGA1, ADE2, and MET25 are nonessential genes in *Y. lipolytica*.^{23,25,35} MGA1 deletion suppresses pseudo hyphal growth in *Y. lipolytica*,²⁷ ADE2 knockout was previously used to evaluate the HR efficiency in *Y. lipolytica*,³⁶ and MET25 knockout was previously used to test the MET25 locus as a genetic marker.³⁷ We used a nontargeting gRNA as a control and transformed equal amounts of DNA, then counted the number of colonies on the transformation plate to determine relative toxicity. The base editor resulted in higher transformation efficiency in two- and three-gene edits than Cas9 in both the Δ Ku70 strain and Po1f strain (Figure 2). The low CFU count in Δ Ku70 strain for multiple gene disruptions in the Cas9 plasmid was likely due to the need to repair several double-stranded breaks, this strain's inability to perform NHEJ, and the lack of template for repair by HDR.³¹ Since the nickase base editor relies on single-stranded nicks instead of double-stranded breaks, base editors were less toxic to the cell. When we evaluated the toxicity using the Po1f strain, the nickase base editors were still less toxic than the Cas9-based dsDNA breaks; however, the Cas9-based dsDNA breaks were less harmful to the Po1f strain than to the Δ Ku70 strain because the Po1f strain preferentially performs NHEJ rather than HDR.

2.3. Single Base Edits Are gRNA Expression-Limited but Can Be Highly Efficient in *Y. lipolytica*. Using established gRNA design methods,^{21,22} we tested base editing on three targets using MGA1, ADE2, and MET25 gRNA. The editing efficiency was 33.3% for MGA1 gRNA1, 26.66% for MGA1 gRNA 2, 38% for ADE2 gRNA, and 50% for MET25 gRNA (Figure 1). This design includes 9bp²¹ or 10bp²² nucleotides between tRNA and gRNA. The first seven nucleotides post-tRNA are the chromosomal DNA sequences post-tRNA in the 5s rRNA region. The next two or three nucleotides were added to insert an AvrII²¹ or NsiI²² restriction digest site for easy gRNA cloning; however, previous research has shown that removing intergenic nucleotides between tRNA and gRNA increased the editing efficiency in Cas9-based knockout and integration.³⁰ We applied this finding to the current cytosine base editor and tested the editing efficiency on the same targets using these modified intergenic regions. The base editing efficiency increased to 96% for MGA1 gRNA 1, 100% for MGA1 gRNA 2, 75% for ADE2 gRNA, and 100% for MET25 gRNA

(Figure 3). Further testing of single base edits, including CAN1 and TRP1, edited each with 100% efficiency (Figure

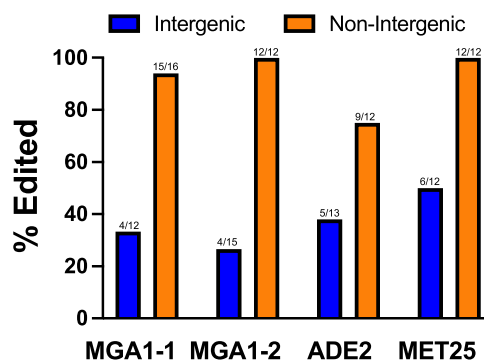


Figure 3. Deleting intergenic nucleotides between tRNA and gRNA increases base editing efficiency in the Δ Ku70 strain. The data is based on the average of at least 12 colonies generated from Sanger sequencing. The number of base edited clones from the total clones is displayed at the top of the bar chart. Original intergenic sequence designs are shown in blue and the intergenic region removed is shown in orange. The truncated nucleotides are shown in Figure S2. The clonal variation for the intergenic and nonintergenic design is shown in Table S2.

S1). Previous work has hypothesized that the increase in editing efficiency was due to the absence of secondary structure perturbations of gRNA.³⁰

2.4. Base Editing Can Be Efficiently Multiplexed with Two- and Three-gRNA Design. After improving the editing efficiency and demonstrating highly efficient single-target base editing, we expanded the range to two- and three-gene targets using MGA1, ADE2, and MET25 combinations. We assembled gRNAs targeting the corresponding genes in a monocistronic design, including promoter, tRNA, and terminator for each gRNA. We used the best-performing gRNAs based on the optimized gRNA design listed in Figure 3. The editing efficiency was 100% for MGA1-ADE2, 83% for MGA1-MET25, and 83% for MGA1-ADE2-MET25 (Figure 4). These multiplexed editing efficiencies are much greater than other multiplex editing efficiencies in *Y. lipolytica*, which were in the 40% range for 3 targets.^{26,27}

We tested multiplexed base editing with polycistronic tRNA-based base editing to simplify the DNA assembly process. This construct had one RNA Pol III promoter driving two gRNAs flanked by tRNA^{gly}. We labeled the native sequences before tRNA^{gly} as the leader sequence and added the leader sequence to the polycistronic base editing. We tested the polycistronic base editing using gRNAs targeting MGA1 and ADE2 with different leader designs. We found that the editing efficiency depended on the leader sequence for the tRNA-based base editing. The editing efficiency increased for two-gene targets as the leader sequence was changed from no leader to a 17nt leader sequence. The editing efficiency for 6nt and 17nt leader sequences was comparable to that for monocistronic two-gene targets (Figure S2). We hypothesize that the increase in editing efficiency caused by the leader sequence change is due to RNase P's increase in cleavage efficiency.³⁸ However, the editing efficiency decreased to 8.3% for three-gene targets with a 17nt leader sequence, suggesting inefficient processing of polycistronic transcripts (Figure S3).

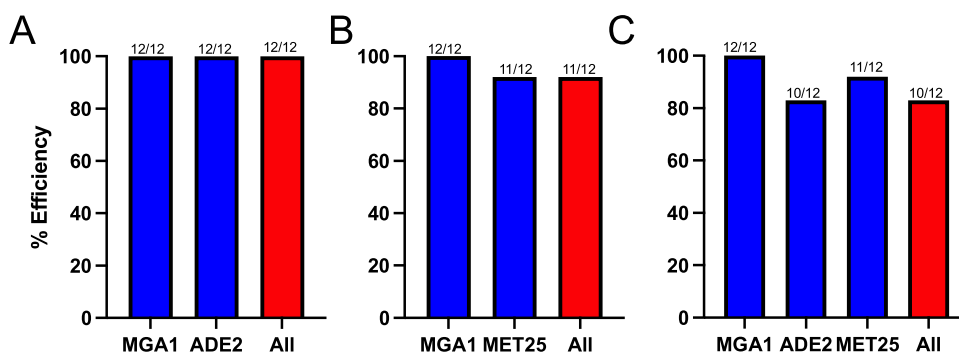


Figure 4. High-efficiency multiplexed editing can be performed up to three targets with the optimized gRNA design in the Δ Ku70 strain. The data is based on an average of at least 12 colonies generated from Sanger sequencing. The number of base edited clones out of total clones is displayed at the top of the bar chart. (A) Editing efficiency of individual gRNAs and overall multiplexed editing efficiency in MGA1-ADE2 multiplexed base editing. (B) Editing efficiency of individual gRNAs and overall multiplexed editing efficiency in MGA1-MET25 multiplexed base editing. (C) Editing efficiency of individual gRNAs and overall multiplexed editing efficiency in MGA1-ADE2-MET25 multiplexed base editing. The clonal variation for the two- and three-gene multiplexed base editing is shown in Table S3.

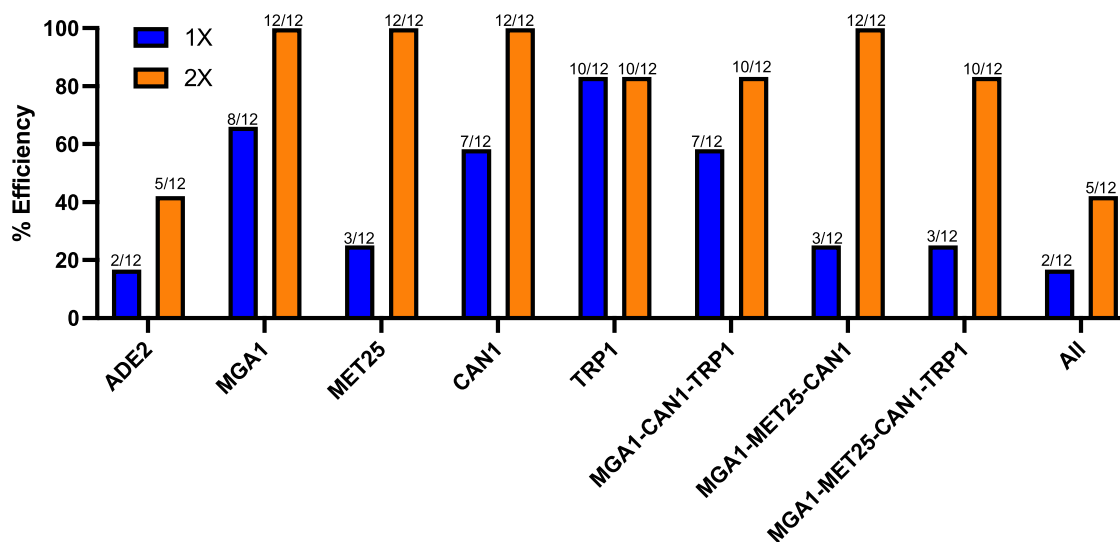


Figure 5. Increasing the copy number increases 5-gene multiplexed base editing efficiency in the Δ Ku70 strain. The data is based on Sanger sequencing from at least 12 colonies. The number of base edited clones from the total clones is displayed at the top of the bar chart. The editing efficiency on 5-gene targets MGA1-ADE2-MET25-CAN1-TRP1 with one copy of base editor and gRNA is shown in blue, and the editing efficiency on 5-gene targets MGA1-ADE2-MET25-CAN1-TRP1 with two copies of the base editor and gRNA is shown in orange. The clonal variation for the 5-gene base editing is shown in Table S4.

2.5. Efficient Multiplexing of 5-Gene Base Edits Is Enabled by Increasing Base Editor and gRNA Expression Level. We expanded multiplexed base editing to up to five genes simultaneously, choosing MGA1, ADE2, MET25, CAN1, and TRP1. Initially, multiplexed editing of three and four genes was 60 and 25% for MGA1-CAN1-TRP1 and MGA1-MET25-CAN1-TRP1, respectively (Figure 5 A). The single gRNA editing for MGA1, ADE2, MET25, CAN1, and TRP1 was 96, 75, 100, 100, and 100% respectively (Figure 3). The overall five-gene editing efficiency was 16.3% for these targets (Figure 5A). Since individual base editing efficiency exceeded the efficiency of multiplexed base editing efficiency at the same sites, we hypothesized that increasing the base editor's and gRNAs' expression levels would improve multiplexed base editing efficiency. We inserted two copies of the base editor (PmCDA1-nCas9-UGI) and of a five-gene gRNA cassette into the genomes, which increased the multiplexed editing efficiency to 42% for the five genes. The three-gene and four-gene multiplexed editing was 100 and 83% for MGA1-CAN1-

TRP1 and MGA1-MET25-CAN1-TRP1, respectively, with two copies of base editor and gRNA (Figure 5).

2.6. CAN1 Co-Selection Enables Efficient Multiplexed Base Editing in Po1f Strain. In previous studies, the base editor was effective in the Δ Ku70 strain but not the commonly used WT Po1f strain.²⁹ In our hands, we also did not observe any base editing with the original gRNA design and only achieved 8.3% base editing efficiency on two-gene targets in the Po1f strain after using the optimized gRNA design (Figure S5). Working with the Δ Ku70 strain can be problematic due to growth defect arising from weakened DNA damage response and lowered metabolic performance.³⁹ Therefore, we wanted to increase the base editing efficiency in the Po1f strain. We used a co-selection approach, where the selection-based enriched editing at one locus simultaneously increases the editing in unrelated genetic loci. Co-selection has been used previously to increase editing efficiency by editing the target locus and receptor for diphtheria toxin (DT), where base edited cells gain resistance to DT toxin,⁴⁰ and in CRISPR

pooled screens for probing fitness effects in *S. cerevisiae*.⁴¹ We used the CAN1 knockout for co-selection because it produced gene edits with 100% efficiency when selected with canavanine in both Po1f and Δ Ku70 strains (Figure S6). Canavanine is a toxic molecule that causes cell death when it enters the cell by the CAN1 importer; thus, CAN1 knockouts confer canavanine resistance.

We tested the base editor's activity in Po1f with both nCas9(D10A) and dCas9(D10A H840A) (Supporting Figure 5). We individually targeted MGA1, ADE2, and MET25 with unoptimized gRNAs and paired them with CAN1 gRNA, and we achieved 100% base editing efficiency (Figure S7). We used gRNAs targeting MGA1, ADE2, MET25, and CAN1 to test the co-selection approach in multiplexed base editing in the Po1f strain. The multiplexed editing efficiency was 40% on MGA1-ADE2-MET25-CAN1, similar to the current lbCpf1 and AsCpf1 systems that multiplex three targets (Figure 6).

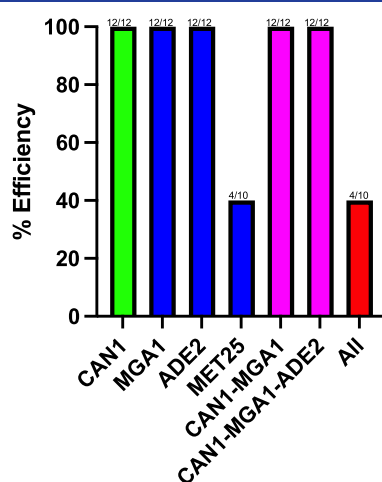


Figure 6. CAN1 co-selection increases multiplexed editing efficiency in Po1f strain. The data are based on an average of 10 colonies generated from Sanger sequencing. The number of base edited clones from the total clones is provided at the top of the bar chart. Multiplexed base editing efficiency on MGA1-ADE2-MET25-CAN1 paired with CAN1 co-selection in Po1f strain. The editing efficiency on MGA1-MET25 without co-selection is shown in Figure S5. The clonal variation for the CAN1 co-selection is shown in Table S5.

The editing efficiency was 100% on two-gene targets, MGA1-ADE2 in three-gene editing (Figure 6). The increase in editing efficiency with CAN1 co-selection suggests that editing in two different loci is not independent and that a cell could be more or less apt to be edited at a given moment in time.

2.7. Rapid Strain Engineering with Multiplexed Knockouts to Increase Naringenin Production. To demonstrate the application of multiplexed cytosine base editing, we used the base editor to increase the production of the natural product naringenin through multiplex gene knockouts. We chose to knock out genes in the native tyrosine and malonyl-CoA biosynthetic pathways to increase naringenin production (Figure 7). Previous work has improved the naringenin production by overexpressing native genes and using glucose or xylose as the carbon source.^{8,9,42} Our work demonstrates for the first time that knockouts in the malonyl-CoA pathway also increase naringenin production.

Several knockouts in both the tyrosine and malonyl-CoA pathways were designed based on inference from the literature. Double knockouts of DGA1 and DGA2 increased β -farnesene

production by 56% as the lipid content was reduced to 8.72% from 26%.⁴³ The addition of fatty acid inhibitor cerulenin increased naringenin production by 31.2% in engineered strains,⁸ pointing to the significance of fatty acid down-regulation to increase malonyl-CoA-based molecules. GPD1 overexpression was combined with DGA1 overexpression to increase lipid production by 12% compared to overexpressing DGA1.⁴⁴ MLS1 and CIT2 are part of the glyoxylate cycle in the peroxisome and deletion of either increased crocetin production by 50% in *S. cerevisiae*.⁴⁵ In another study, the deletion of CIT2 or MLS1 increased α -santalene production by 36 and 127%, respectively, in *S. cerevisiae*.⁴⁶

We used glycerol and glucose as two carbon sources to evaluate the impact of base editor-based knockouts. When glucose was used as a carbon source, double deletion of MLS and CIT2 resulted in a 2-fold increase in naringenin production compared to that of the wild type (Figure 8). However, the quadruple deletion of DGA1, DGA2, MLS1, and CIT2 showed no increase in naringenin production compared with the double deletion of MLS and CIT2 (Figure 8). This suggests acetyl-CoA accumulation is a bottleneck for naringenin synthesis, not malonyl-CoA's diversion. All of the combinations of multiple deletions involving CIT2 deletion showed an increase in naringenin production compared to the wild type. Quadruple deletion of GPD1, DGA1, DGA2, and CIT2 resulted in a 1.5-fold production increase compared to the wild type. Triple deletions of DGA1, DGA2, and CIT2 resulted in 1.63-fold and 1.73-fold increases compared to the wild type. Double deletion of GPD1 and DGA1 showed no increase compared to that of the wild type (Figure 8). The individual knockouts of DGA1, DGA2, MLS, and CIT2 resulted in no increase compared to the wild type when tested in a culture tube (Figure S10).

When glycerol was used as a carbon source, quadruple deletion of GPD1, DGA1, DGA2, and CIT2 showed a 1.87-fold increase compared with the wild type (Figure 8). All multiple deletions with GPD1 knockout showed an increase in naringenin production compared to the wild type. Double deletion of GPD1 and DGA1, and triple deletion of GPD1, DGA1, and CIT2 showed 1.60- and 1.77-fold increases in naringenin synthesis compared to the wild type. Quadruple deletion of DGA1, DGA2, MLS, and CIT2, and double deletion of MLS and CIT2 showed 1.16- and 1.33-fold changes compared to the wild type, respectively. Triple deletion of DGA1, DGA2, and CIT2 showed no increase in naringenin production compared to that of the wild type (Figure 8).

When multiplexed knockouts were accomplished in the tyrosine module, triple deletion of TRP2, PDT1, and ARO10 showed a 2-fold increase in naringenin production with both glucose and glycerol as the carbon source (Figure 8). The individual knockouts of TRP2, PDT1, and ARO10 showed no increase in naringenin production compared to the wild type when tested in a culture tube (Figure S9).

This is the first report of multiplexed knockouts to increase the number of malonyl-CoA-based molecules in *Y. lipolytica*. We identified MLS1, CIT2, and GPD1 knockouts as important targets for increasing naringenin synthesis with either glucose or glycerol carbon sources. These targets can also be used for other malonyl-CoA-derived small molecules. Overexpression of feedback inhibition-resistant alleles ARO4^{K221L} and ACC1 in the multigene knockouts would further increase naringenin

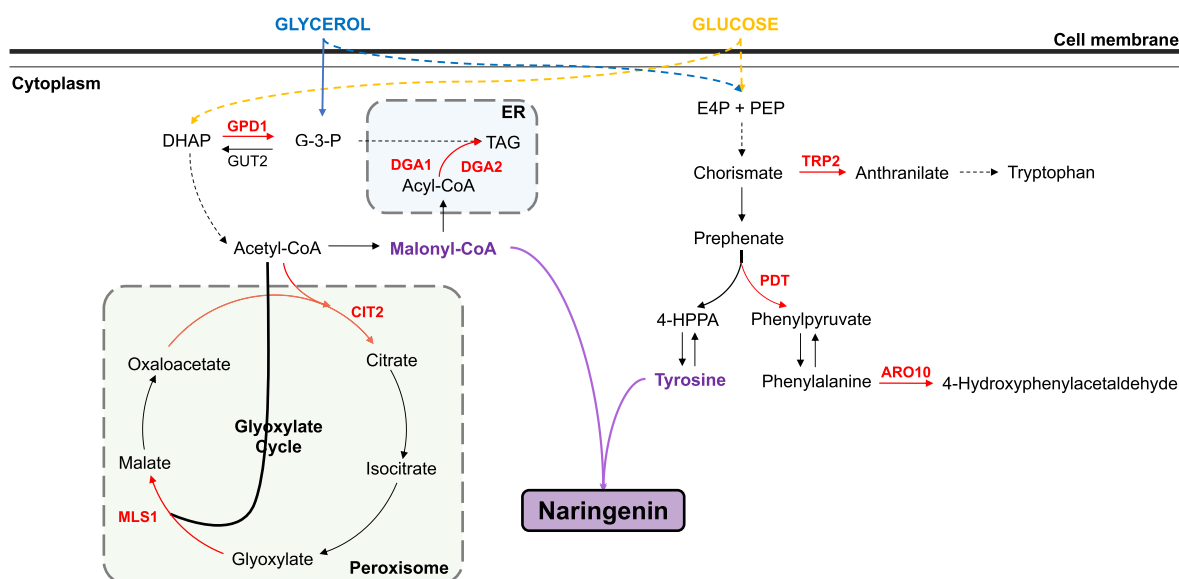


Figure 7. Metabolic pathway for naringenin biosynthesis. Genes targeted for knocking out genes in the malonyl-CoA and tyrosine pathway module to increase the production of natural product naringenin via the tyrosine biosynthetic module and the malonyl-CoA biosynthetic module. Red denotes the knockouts, and purple indicates important precursors.

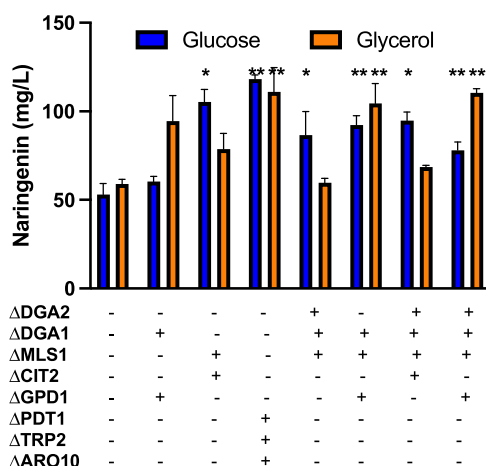


Figure 8. Cytosine base editor for rapid strain engineering with multiplexed knockouts to increase naringenin synthesis with glucose or glycerol as the carbon source. The data are based on an average of three biological replicates. Statistical significance was performed using the Student's two-tailed *t* test. Single asterisk indicates a *p*-value of 0.06–0.10, and double asterisk indicates a *p*-value < 0.05. The error bar denotes the standard error calculated between three biological replicates.

production. The high naringenin-producing strain could be used to produce complex flavonoids further.

Multiplexed editing has been previously done in *S. cerevisiae* up to 8 gene deletions at once.⁴⁷ However, in nonconventional yeasts, our work is the largest number of multiplex gene edits reported to date. When multiplexed gene deletion was accomplished in *S. cerevisiae* by replacing it with a donor on a Cas9 integrated strain, the expression of gRNA was the bottleneck.⁴⁸ Previous work has also identified that gRNA expression was a bottleneck for the CRISPR-based system in *Y. lipolytica*.²¹ However, another study indicated that both the Cas9 and gRNA expression became bottlenecks for multiplexed gene integration, likely due to the titration of Cas9 by several gRNA.⁴⁹ We observed that the expression of gRNA was

the bottleneck for single base edits but that the base editor and gRNA were bottlenecks for 5-gene multiplexed base editing.

Base editing has been difficult in NHEJ-dominant cells. We hypothesize that base editors have not been efficient in NHEJ-dominant cells because a minimal repair is needed as the nicking is being performed, and cytosine is being converted to uracil. Since CAN1 selection only selects cells carrying the canavanine knockouts, the base edited events are enriched in the CAN1 selection experiment. Highly successful co-selection gene editing means that successful base editing events in the same cell are not independent of each other. The mechanism behind how increased editing at one locus increases the editing at another unrelated locus is yet unknown; however, we hypothesize that co-selection does not increase the number of edited events but only makes the unedited events invisible, thus enriching the number of edited events. It is likely that co-selection can also be used in other CRISPR-based gene editing, such as integration and prime editing.

We targeted the two modules feeding naringenin biosynthesis to demonstrate the use of multiplex gene editing for metabolic engineering. The GPD1, DGA1, DGA2, CIT2, MLS1, and TSC13 were targeted for increasing naringenin synthesis in the malonyl-CoA module (Figure 7). We hypothesized GPD1, CIT2, and MLS knockouts would increase malonyl-CoA accumulation by increasing acetyl-CoA availability, whereas DGA1 and DGA2 are targeted to divert the malonyl-CoA flux toward naringenin production from lipids. We observed that the knockouts of DGA1 and DGA2 did not increase naringenin production, contradicting the previous work on β -farnesene production.⁴³ We hypothesize that it is because the knockouts were performed on a strain engineered to possess a high acetyl-CoA flux. We also observed that knockouts of MLS1 and CIT2 increased naringenin production, as hypothesized based on prior work to produce crocetin in *S. cerevisiae*.⁴⁵ No previous work informed our choice of GPD1 knockout; however, we observed that GPD1 knockout increased naringenin production only when glycerol was used as a carbon source. Tsc13 was targeted to prevent the

reported promiscuous activity of Tsc13 on chalcone synthase in *S. cerevisiae*.^{50–53} Even though the base editing efficiency was high, we could not obtain the stop codon mutations in Tsc13 with the base editor (Figure S8). Tsc13 gene encodes for very-long-chain enoyl-CoA reductase, catalyzing the final step in each cycle of long-chain fatty acid elongation. This pointed to a previously unreported essentiality of the Tsc13 gene in *Y. lipolytica*, similar to *S. cerevisiae*.^{54,55}

We also targeted PDT, TRP2, and ARO10 to increase the tyrosine flux (Figure 7). They were hypothesized to increase the accumulation of tyrosine, a key precursor to naringenin. Previously, double deletion of PDT and ARO10 showed a 3-fold increase in naringenin synthesis in *S. cerevisiae* while decreasing the accumulation of 2-phenyl ethanol.⁵⁶ TRP2 was hypothesized to decrease the tryptophan accumulation, thereby increasing the tyrosine flux. Our observed increase in naringenin production with multiple knockouts of PDT, TRP2, and ARO10 is consistent with this previous work in *S. cerevisiae*.⁵⁶

3. CONCLUSIONS

In conclusion, a multiplexed cytosine base editor will be a valuable addition to the synthetic biology toolbox of *Y. lipolytica*. We have demonstrated that the cytosine base editor can perform multiplexed gene editing efficiently, irrespective of the strains. The editing efficiency exceeds the current multiplexed gene editing methods in *Y. lipolytica*. We also demonstrated the application of a cytosine base editor by rapid multiplexed gene editing to increase naringenin production, identifying novel targets for increasing malonyl-CoA-derived molecules.

4. MATERIALS AND METHODS

4.1. Strains and Media. The Δ Ku70 strain was generated by knocking out the Ku70 gene from the wild-type Polf (ATCCMYA2163).³¹ The Δ Ku70 strain was used for base editing experiments, unless specified. YSC-URA medium supplemented with 2% glucose was used for all of the base editor experiments except the two-copy base editor experiment. YSC-LEU-URA medium supplemented with 2% glucose was used for the two-copy base editor experiments. The liquid transformants were plated on a nonselective YSC plate supplemented with 2% glucose to evaluate base editing efficiency. For CAN1 co-selection experiments, liquid transformants were plated on YSC-arginine supplemented with 2% glucose and 80 mg/L L-canavanine (Sigma-Aldrich). Naringenin fermentation was done in 50 mL baffled flasks containing 12 mL YP (2% yeast extract and 1% peptone) media supplemented with 2% glucose or glycerol at 30 °C. Precultures were inoculated at an initial OD of 0.05. Naringenin extraction was done at 84 h. LB media supplemented with 100 μ g/L ampicillin or 50 μ g/mL kanamycin was used for cloning. All cultures were cultured in a 14 mL polystyrene tube containing 2 mL of liquid culture. Yeast cultures were grown at 30 °C and 215 rpm.

4.2. Plasmid Design and Cloning. Cytosine deaminase from *Petromyza marinus* and uracil glycosylase inhibitor from *Bacillus subtilis* bacteriophage PBS1 were codon-optimized for *Y. lipolytica* by Genscript's Gensmart tool and synthesized as gene fragments by Genewiz. PmCDA1 was fused to the N-terminus of nCas9(D10A) using the 48bp XTEN linker, and UGI was fused to the C-terminus of nCas9(D10A) using the

SGGS linker. The NLS tag was fused to UGI through the linker SRAD. The PIW(URA) uracil plasmid was digested with AscI and NheI, and three fragments were inserted by using the NEBHiFi DNA Assembly master mix. FjTAL, A4CL, PhCHS, and MsCHI were codon-optimized by Genscript's Gensmart tool using *Y. lipolytica* and synthesized as gene fragments by Genscript. FjTAL-At4CL-MsCHI was integrated at the AXP locus of the Δ Ku70 strain. PhCHS was integrated at the D17 locus in AXP (FjTAL-At4CL-MsCHI). All of the plasmids and primers for assembly are listed in Table S11. All of the codon-optimized gene sequences are listed in Table S14.

4.3. Plasmid Design for Golden Gate Base Editor Vector. First, the base editor plasmid was modified to insert type IIs BsmBI sites at the end of tRNA^{gly} and the beginning of the poly T terminator. A template containing gRNA scaffold-Poly T-Scrp'-tRNA^{gly} was constructed in the kanamycin plasmid backbone. gRNAs were inserted through PCR amplification in which overhangs constituted 20bp gRNA sequences. The overhangs were split between forward and reverse primers according to the 4bp sticky ends. The primers used for single gRNA cloning are listed in Table S9. The primers used for multiplexed gRNA cloning are listed in Supporting Table S10.

4.4. gRNA Design for Base Editor. gRNA was designed using a genome web portal using *Y. lipolytica* as the species of interest.³² Cytosine or guanine was identified in the 4bp window starting C15–C18 from the PAM sequence. gRNAs were selected as those without any off-target effects. gRNAs were designed to target the coding strand of genes containing CGA (Arg), CAG (Gln), CAA (Gln), and TGG (Trp) to create stop codons. All of the gRNAs used in this study are as described in Table S5.

4.5. Yeast Transformation. 1000 ng episomal DNA carrying base editor and gRNA was transformed in 200 μ L yeast transformation mix containing 40% PEG4000, 0.1 M dithiothreitol, 0.1 M Lithium acetate, and 250 ng boiled salmon sperm DNA. A loop of cells (approximately 10⁸ cells) from the YPD plate was added to the yeast transformation mix and heat-shocked for 90 min at 39 °C. 700 μ L of YSC-LEU media or YSC-LEU-URA media was added and centrifuged at 5000g for 5 min. The supernatant was removed, and the cell pellet was resuspended with 1 mL of YSC-LEU or YSC-LEU-URA media. The resuspend mix was added to 1 mL of drop-out media and was grown in a 28 °C shaker at 215 rpm for 72 h. 20 μ L of the preculture was added to 2 mL of YSC-LEU or YSC-LEU-URA media and grown for 48 h. 3 μ L of culture was added to 1 mL of sterile water and plated in the nonselective plate with 15 or 125 μ L. For CAN1 co-selection experiments, the culture was plated in a YSC-Arginine plate containing 80 mg/L of canavanine. Colonies from every plate were picked, PCR amplified, and sent for Sanger sequencing (Genewiz).

4.6. Golden Gate Assembly Protocol. Golden Gate assembly was used for cloning guide RNAs. Domestication of BsmBI sites was done using Gibson assembly protocol at three different regions of the plasmid. A template containing a gRNA scaffold was used for cloning single guide RNAs. Overhangs on the forward primer contained the 20bp gRNA sequences for targeting the genes. A template containing scaffold-Scrp-tRNA and scaffolds was used to assemble multiple gRNAs. Overhangs on the primers were used to insert 20bp guide RNAs. The overhangs were split up into forward or reverse primers based on 4bp sticky ends. Different sticky ends were used at each junction. Golden gate assembly was done by using the

NEBBridge ligase master mix's protocol. All of the Golden Gate assembly reactions were done at 60 °C for 5 min and 16 °C for 5 min, followed by final 60 °C incubation for 1 h. 2.5 μ L of the Golden Gate mix was transformed with 50 μ L of DH5- α competent cells. Q5 Hot Start PCR master mix(2X) was used for PCR, and clones were verified by Sanger sequencing with Genewiz.

4.7. High-Performance Liquid Chromatography (HPLC) for Naringenin Quantification. 1 mL methanol was added to 1 mL of cell culture and sonicated for 60 min. The sonicated mix was centrifuged at 12,000g for 20 min, and 10 μ L of the extract was run on Agilent 1200 HPLC equipped with a variable detector and C18 column (Agilent RRHD Eclipse Plus C18, 2.1 \times 50 mm², 1.8 μ m). The gradient method was used at a flow rate of 0.5 mL/min using water (Solvent A) and acetonitrile (Solvent B) with the following method: start at 5% B, hold at 5% B for 1.5 min, 10% B to 99% B for 12 min, hold at 99% B for 3 min, and 99% B to 5% B for 1 min; the total run time was 16 min. Naringenin was detected at a retention time of 5.5 min at a wavelength of 290 nm.

■ ASSOCIATED CONTENT

SI Supporting Information

The Supporting Information is available free of charge at <https://pubs.acs.org/doi/10.1021/acssynbio.3c00435>.

Impact of cytosine base editor-based knockouts and comparison between intergenic and non-intergenic gRNA designs (Figures S1–S10) and base editing efficiency and primers (Tables S1–S14) (PDF)

■ AUTHOR INFORMATION

Corresponding Author

Mark Blenner – Department of Chemical & Biomolecular Engineering, University of Delaware, Newark, Delaware 19716, United States; orcid.org/0000-0001-9274-3749; Email: Blenner@udel.edu

Authors

Vijaydev Ganesan – Department of Chemical & Biomolecular Engineering, University of Delaware, Newark, Delaware 19716, United States

Lummy Monteiro – Department of Chemical & Biomolecular Engineering, University of Delaware, Newark, Delaware 19716, United States

Dheeraj Pedada – Department of Chemical & Biomolecular Engineering, University of Delaware, Newark, Delaware 19716, United States

Anthony Stohr – Department of Chemical & Biomolecular Engineering, University of Delaware, Newark, Delaware 19716, United States; orcid.org/0000-0002-2388-1723

Complete contact information is available at: <https://pubs.acs.org/doi/10.1021/acssynbio.3c00435>

Author Contributions

V.G.: conceptualization, methodology, validation, formal analysis, investigation, writing—original and draft, writing—review and editing, visualization. L.M.: formal analysis, investigation, writing—review and editing, visualization. D.P.: validation, investigation, writing—review and editing. A.S.: investigation, writing—review and editing. M.B.: conceptualization, methodology, resources, writing—original and draft,

writing—review and editing, visualization, supervision, project administration, funding acquisition.

Notes

The authors declare no competing financial interest.

■ ACKNOWLEDGMENTS

The authors thank Dr. Jaya Singh, Spencer Grissom, and Derron Ma for reviewing the manuscript. Research reported in this publication was supported by the National Institute of General Medical Sciences of the National Institutes of Health under award number R35GM133803

■ REFERENCES

- (1) Qiao, K.; Abidi, S. H. I.; Liu, H.; Zhang, H.; Chakraborty, S.; Watson, N.; Ajikumar, P. K.; Stephanopoulos, G. Engineering Lipid Overproduction in the Oleaginous Yeast *Yarrowia Lipolytica*. *Metab. Eng.* **2015**, *29*, 56–65.
- (2) Rodriguez, G. M.; Hussain, M. S.; Gambill, L.; Gao, D.; Yaguchi, A.; Blenner, M. Engineering Xylose Utilization in *Yarrowia Lipolytica* by Understanding Its Cryptic Xylose Pathway. *Biotechnol. Biofuels* **2016**, *9* (1), No. 149.
- (3) Brabender, M.; Hussain, M. S.; Rodriguez, G.; Blenner, M. A. Urea and Urine Are a Viable and Cost-Effective Nitrogen Source for *Yarrowia Lipolytica* Biomass and Lipid Accumulation. *Appl. Microbiol. Biotechnol.* **2018**, *102* (5), 2313–2322.
- (4) Qiao, K.; Wasylenko, T. M.; Zhou, K.; Xu, P.; Stephanopoulos, G. Lipid Production in *Yarrowia Lipolytica* Is Maximized by Engineering Cytosolic Redox Metabolism. *Nat. Biotechnol.* **2017**, *35* (2), 173–177.
- (5) Xue, Z.; Sharpe, P. L.; Hong, S.-P.; Yadav, N. S.; Xie, D.; Short, D. R.; Damude, H. G.; Rupert, R. A.; Seip, J. E.; Wang, J.; Pollak, D. W.; Bostick, M. W.; Bosak, M. D.; Macool, D. J.; Hollerbach, D. H.; Zhang, H.; Arcilla, D. M.; Bledsoe, S. A.; Croker, K.; McCord, E. F.; Tyreus, B. D.; Jackson, E. N.; Zhu, Q. Production of Omega-3 Eicosapentaenoic Acid by Metabolic Engineering of *Yarrowia Lipolytica*. *Nat. Biotechnol.* **2013**, *31* (8), 734–740.
- (6) Cordova, L. T.; Butler, J.; Alper, H. S. Direct Production of Fatty Alcohols from Glucose Using Engineered Strains of *Yarrowia Lipolytica*. *Metab. Eng. Commun.* **2020**, *10*, No. e00105.
- (7) Wang, G.; Xiong, X.; Ghogare, R.; Wang, P.; Meng, Y.; Chen, S. Exploring Fatty Alcohol-Producing Capability of *Yarrowia Lipolytica*. *Biotechnol. Biofuels* **2016**, *9* (1), No. 107.
- (8) Lv, Y.; Marsafari, M.; Koffas, M.; Zhou, J.; Xu, P. Optimizing Oleaginous Yeast Cell Factories for Flavonoids and Hydroxylated Flavonoids Biosynthesis. *ACS Synth. Biol.* **2019**, *8* (11), 2514–2523.
- (9) Palmer, C. M.; Miller, K. K.; Nguyen, A.; Alper, H. S. Engineering 4-Coumaroyl-CoA Derived Polyketide Production in *Yarrowia Lipolytica* through a β -Oxidation Mediated Strategy. *Metab. Eng.* **2020**, *57*, 174–181.
- (10) Ma, Y.; Liu, N.; Greisen, P.; Li, J.; Qiao, K.; Huang, S.; Stephanopoulos, G. Removal of Lycopene Substrate Inhibition Enables High Carotenoid Productivity in *Yarrowia Lipolytica*. *Nat. Commun.* **2022**, *13* (1), No. 572.
- (11) Jacobsen, I. H.; Ledesma-Amaro, R.; Martinez, J. L. Recombinant β -Carotene Production by *Yarrowia Lipolytica* – Assessing the Potential of Micro-Scale Fermentation Analysis in Cell Factory Design and Bioreaction Optimization. *Front. Bioeng. Biotechnol.* **2020**, *8*, No. 29.
- (12) Shabbir Hussain, M.; Gambill, L.; Smith, S.; Blenner, M. A. Engineering Promoter Architecture in Oleaginous Yeast *Yarrowia Lipolytica*. *ACS Synth. Biol.* **2016**, *5* (3), 213–223.
- (13) Blazeck, J.; Liu, L.; Redden, H.; Alper, H. Tuning Gene Expression in *Yarrowia Lipolytica* by a Hybrid Promoter Approach. *Appl. Environ. Microbiol.* **2011**, *77* (22), 7905–7914.
- (14) Trassaert, M.; Vandermies, M.; Carly, F.; Denies, O.; Thomas, S.; Fickers, P.; Nicaud, J.-M. New Inducible Promoter for Gene

Expression and Synthetic Biology in *Yarrowia Lipolytica*. *Microb. Cell Fact* **2017**, *16* (1), No. 141.

(15) Shabbir Hussain, M.; Wheeldon, I.; Blenner, M. A. A Strong Hybrid Fatty Acid Inducible Transcriptional Sensor Built From *Yarrowia Lipolytica* Upstream Activating and Regulatory Sequences. *Biotechnol. J.* **2017**, *12* (10), No. 1700248.

(16) Xiong, X.; Chen, S. Expanding Toolbox for Genes Expression of *Yarrowia Lipolytica* to Include Novel Inducible, Repressible, and Hybrid Promoters. *ACS Synth. Biol.* **2020**, *9* (8), 2208–2213.

(17) Larroude, M.; Park, Y.; Soudier, P.; Kubiak, M.; Nicaud, J.; Rossignol, T. A Modular Golden Gate Toolkit for *Yarrowia Lipolytica* Synthetic Biology. *Microb. Biotechnol.* **2019**, *12* (6), 1249–1259.

(18) Celińska, E.; Ledesma-Amaro, R.; Larroude, M.; Rossignol, T.; Pauthenier, C.; Nicaud, J.-M. Golden Gate Assembly System Dedicated to Complex Pathway Manipulation in *Yarrowia Lipolytica*. *Microb. Biotechnol.* **2017**, *10* (2), 450–455.

(19) Li, Y.-W.; Yang, C.-L.; Shen, Q.; Peng, Q.-Q.; Guo, Q.; Nie, Z.-K.; Sun, X.-M.; Shi, T.-Q.; Ji, X.-J.; Huang, H. YALlcloneNHEJ: An Efficient Modular Cloning Toolkit for NHEJ Integration of Multigene Pathway and Terpenoid Production in *Yarrowia Lipolytica*. *Front. Bioeng. Biotechnol.* **2022**, *9*, No. 816980.

(20) Tong, Y.; Zhou, J.; Zhang, L.; Xu, P. A Golden-Gate Based Cloning Toolkit to Build Viologen Pathway Libraries in *Yarrowia Lipolytica*. *ACS Synth. Biol.* **2021**, *10* (1), 115–124.

(21) Schwartz, C. M.; Hussain, M. S.; Blenner, M.; Wheeldon, I. Synthetic RNA Polymerase III Promoters Facilitate High-Efficiency CRISPR–Cas9-Mediated Genome Editing in *Yarrowia Lipolytica*. *ACS Synth. Biol.* **2016**, *5* (4), 356–359.

(22) Gao, D.; Smith, S.; Spagnuolo, M.; Rodriguez, G.; Blenner, M. Dual CRISPR-Cas9 Cleavage Mediated Gene Excision and Targeted Integration in *Yarrowia Lipolytica*. *Biotechnol. J.* **2018**, *13* (9), No. 1700590.

(23) Schwartz, C.; Cheng, J.-F.; Evans, R.; Schwartz, C. A.; Wagner, J. M.; Anglin, S.; Beitz, A.; Pan, W.; Lonardi, S.; Blenner, M.; Alper, H. S.; Yoshikuni, Y.; Wheeldon, I. Validating Genome-Wide CRISPR-Cas9 Function Improves Screening in the Oleaginous Yeast *Yarrowia Lipolytica*. *Metab. Eng.* **2019**, *55*, 102–110.

(24) Gao, S.; Tong, Y.; Wen, Z.; Zhu, L.; Ge, M.; Chen, D.; Jiang, Y.; Yang, S. Multiplex Gene Editing of the *Yarrowia Lipolytica* Genome Using the CRISPR-Cas9 System. *J. Ind. Microbiol. Biotechnol.* **2016**, *43* (8), 1085–1093.

(25) Baisya, D.; Ramesh, A.; Schwartz, C.; Lonardi, S.; Wheeldon, I. Genome-Wide Functional Screens Enable the Prediction of High Activity CRISPR-Cas9 and -Cas12a Guides in *Yarrowia Lipolytica*. *Nat. Commun.* **2022**, *13* (1), No. 922.

(26) Yang, Z.; Edwards, H.; Xu, P. CRISPR-Cas12a/Cpf1-Assisted Precise, Efficient and Multiplexed Genome-Editing in *Yarrowia Lipolytica*. *Metab. Eng. Commun.* **2020**, *10*, No. e00112.

(27) Ramesh, A.; Ong, T.; Garcia, J. A.; Adams, J.; Wheeldon, I. Guide RNA Engineering Enables Dual Purpose CRISPR-Cpf1 for Simultaneous Gene Editing and Gene Regulation in *Yarrowia Lipolytica*. *ACS Synth. Biol.* **2020**, *9* (4), 967–971.

(28) Borsenberger, V.; Croux, C.; Daboussi, F.; Neuvéglise, C.; Bordes, F. Developing Methods to Circumvent the Conundrum of Chromosomal Rearrangements Occurring in Multiplex Gene Edition. *ACS Synth. Biol.* **2020**, *9* (9), 2562–2575.

(29) Bae, S.; Park, B. G.; Kim, B.; Hahn, J. Multiplex Gene Disruption by Targeted Base Editing of *Yarrowia Lipolytica* Genome Using Cytidine Deaminase Combined with the CRISPR/Cas9 System. *Biotechnol. J.* **2020**, *15* (1), No. 1900238.

(30) Abdel-Mawgoud, A. M.; Stephanopoulos, G. Improving CRISPR/Cas9-Mediated Genome Editing Efficiency in *Yarrowia Lipolytica* Using Direct TRNA-SgRNA Fusions. *Metab. Eng.* **2020**, *62*, 106–115.

(31) Verbeke, J.; Beopoulos, A.; Nicaud, J.-M. Efficient Homologous Recombination with Short Length Flanking Fragments in Ku70 Deficient *Yarrowia Lipolytica* Strains. *Biotechnol. Lett.* **2013**, *35* (4), 571–576.

(32) Hwang, G.-H.; Park, J.; Lim, K.; Kim, S.; Yu, J.; Yu, E.; Kim, S.-T.; Eils, R.; Kim, J.-S.; Bae, S. Web-Based Design and Analysis Tools for CRISPR Base Editing. *BMC Bioinf.* **2018**, *19* (1), No. 542.

(33) Schwartz, C.; Curtis, N.; Löbs, A.-K.; Wheeldon, I. Multiplexed CRISPR Activation of Cryptic Sugar Metabolism Enables *Yarrowia Lipolytica* Growth on Cellobiose. *Biotechnol. J.* **2018**, *13* (9), No. 1700584.

(34) Schwartz, C.; Frogue, K.; Ramesh, A.; Misa, J.; Wheeldon, I. CRISPRi Repression of Nonhomologous End-joining for Enhanced Genome Engineering via Homologous Recombination in *Yarrowia Lipolytica*. *Biotechnol. Bioeng.* **2017**, *114* (12), 2896–2906.

(35) Patterson, K.; Yu, J.; Landberg, J.; Chang, I.; Shavarebi, F.; Bilanchone, V.; Sandmeyer, S. Functional Genomics for the Oleaginous Yeast *Yarrowia Lipolytica*. *Metab. Eng.* **2018**, *48*, 184–196.

(36) Ji, Q.; Mai, J.; Ding, Y.; Wei, Y.; Ledesma-Amaro, R.; Ji, X.-J. Improving the Homologous Recombination Efficiency of *Yarrowia Lipolytica* by Grafting Heterologous Component from *Saccharomyces Cerevisiae*. *Metab. Eng. Commun.* **2020**, *11*, No. e00152.

(37) Edwards, H.; Yang, Z.; Xu, P. Characterization of Met25 as a Color Associated Genetic Marker in *Yarrowia Lipolytica*. *Metab. Eng. Commun.* **2020**, *11*, No. e00147.

(38) Xie, K.; Minkenberg, B.; Yang, Y. Boosting CRISPR/Cas9 Multiplex Editing Capability with the Endogenous TRNA-Processing System. *Proc. Natl. Acad. Sci. U.S.A.* **2015**, *112* (11), 3570–3575.

(39) Ploessl, D.; Zhao, Y.; Cao, M.; Ghosh, S.; Lopez, C.; Sayadi, M.; Chudalayandi, S.; Severin, A.; Huang, L.; Gustafson, M.; Shao, Z. A Repackaged CRISPR Platform Increases Homology-Directed Repair for Yeast Engineering. *Nat. Chem. Biol.* **2022**, *18* (1), 38–46.

(40) Li, S.; Akrap, N.; Cerboni, S.; Porritt, M. J.; Wimberger, S.; Lundin, A.; Möller, C.; Firth, M.; Gordon, E.; Lazovic, B.; Sieńska, A.; Pane, L. S.; Coelho, M. A.; Ciotta, G.; Pellegrini, G.; Sini, M.; Xu, X.; Mitra, S.; Bohlooly-Y, M.; Taylor, B. J. M.; Sienski, G.; Maresca, M. Universal Toxin-Based Selection for Precise Genome Engineering in Human Cells. *Nat. Commun.* **2021**, *12* (1), No. 497.

(41) Després, P. C.; Dubé, A. K.; Nielly-Thibault, L.; Yachie, N.; Landry, C. R. Double Selection Enhances the Efficiency of Target-AID and Cas9-Based Genome Editing in Yeast. *G3: Genes, Genomes, Genetics* **2018**, *8* (10), 3163–3171.

(42) Wei, W.; Zhang, P.; Shang, Y.; Zhou, Y.; Ye, B.-C. Metabolically Engineering of *Yarrowia Lipolytica* for the Biosynthesis of Naringenin from a Mixture of Glucose and Xylose. *Bioresour. Technol.* **2020**, *314*, No. 123726.

(43) Liu, Y.; Zhang, J.; Li, Q.; Wang, Z.; Cui, Z.; Su, T.; Lu, X.; Qi, Q.; Hou, J. Engineering *Yarrowia Lipolytica* for the Sustainable Production of β -Farnesene from Waste Oil Feedstock. *Biotechnol. Biofuels* **2022**, *15* (1), 101.

(44) Friedlander, J.; Tsakraklides, V.; Kamineni, A.; Greenhagen, E. H.; Consiglio, A. L.; MacEwen, K.; Crabtree, D. V.; Afshar, J.; Nugent, R. L.; Hamilton, M. A.; Joe Shaw, A.; South, C. R.; Stephanopoulos, G.; Brevnova, E. E. Engineering of a High Lipid Producing *Yarrowia Lipolytica* Strain. *Biotechnol. Biofuels* **2016**, *9* (1), 77.

(45) Song, T.; Wu, N.; Wang, C.; Wang, Y.; Chai, F.; Ding, M.; Li, X.; Yao, M.; Xiao, W.; Yuan, Y. Crocetin Overproduction in Engineered *Saccharomyces Cerevisiae* via Tuning Key Enzymes Coupled With Precursor Engineering. *Front. Bioeng. Biotechnol.* **2020**, *8*, No. 578005.

(46) Chen, Y.; Daviet, L.; Schalk, M.; Siewers, V.; Nielsen, J. Establishing a Platform Cell Factory through Engineering of Yeast Acetyl-CoA Metabolism. *Metab. Eng.* **2013**, *15*, 48–54.

(47) Zhang, Y.; Wang, J.; Wang, Z.; Zhang, Y.; Shi, S.; Nielsen, J.; Liu, Z. A GRNA-TRNA Array for CRISPR-Cas9 Based Rapid Multiplexed Genome Editing in *Saccharomyces Cerevisiae*. *Nat. Commun.* **2019**, *10* (1), No. 1053.

(48) Horwitz, A. A.; Walter, J. M.; Schubert, M. G.; Kung, S. H.; Hawkins, K.; Platt, D. M.; Hernday, A. D.; Mahatdejkul-Meadows, T.; Szeto, W.; Chandran, S. S.; Newman, J. D. Efficient Multiplexed Integration of Synergistic Alleles and Metabolic Pathways in Yeasts via CRISPR-Cas. *Cell Syst.* **2015**, *1* (1), 88–96.

(49) Bao, Z.; Xiao, H.; Liang, J.; Zhang, L.; Xiong, X.; Sun, N.; Si, T.; Zhao, H. Homology-Integrated CRISPR–Cas (HI-CRISPR) System for One-Step Multigene Disruption in *Saccharomyces Cerevisiae*. *ACS Synth. Biol.* **2015**, *4* (5), 585–594.

(50) Kong, D.; Li, S.; Smolke, C. D. Discovery of a Previously Unknown Biosynthetic Capacity of Naringenin Chalcone Synthase by Heterologous Expression of a Tomato Gene Cluster in Yeast. *Sci. Adv.* **2020**, *6* (44), No. eabd1143.

(51) Lehka, B. J.; Eichenberger, M.; Bjørn-Yoshimoto, W. E.; Vanegas, K. G.; Buijs, N.; Jensen, N. B.; Dyekjær, J. D.; Jenssen, H.; Simon, E.; Naesby, M. Improving Heterologous Production of Phenylpropanoids in *Saccharomyces Cerevisiae* by Tackling an Unwanted Side Reaction of Tsc13, an Endogenous Double Bond Reductase. *FEMS Yeast Res.* **2017**, No. fox004.

(52) Liu, D.; Sica, M. S.; Mao, J.; Chao, L. F.-I.; Siewers, V. A *p*-Coumaroyl-CoA Biosensor for Dynamic Regulation of Naringenin Biosynthesis in *Saccharomyces Cerevisiae*. *ACS Synth. Biol.* **2022**, *11* (10), 3228–3238.

(53) Tous Mohedano, M.; Mao, J.; Chen, Y. Optimization of Pinocembrin Biosynthesis in *Saccharomyces Cerevisiae*. *ACS Synth. Biol.* **2023**, *12* (1), 144–152.

(54) Sanz, A. B.; Díez-Muñiz, S.; Moya, J.; Petryk, Y.; Nombela, C.; Rodríguez-Peña, J. M.; Arroyo, J. Systematic Identification of Essential Genes Required for Yeast Cell Wall Integrity: Involvement of the RSC Remodelling Complex. *JoF* **2022**, *8* (7), No. 718.

(55) Kohlwein, S. D.; Eder, S.; Oh, C.-S.; Martin, C. E.; Gable, K.; Bacikova, D.; Dunn, T. Tsc13p Is Required for Fatty Acid Elongation and Localizes to a Novel Structure at the Nuclear-Vacuolar Interface in *Saccharomyces Cerevisiae*. *Mol. Cell. Biol.* **2001**, *21* (1), 109–125.

(56) Koopman, F.; Beekwilder, J.; Crimi, B.; van Houwelingen, A.; Hall, R. D.; Bosch, D.; van Maris, A. J.; Pronk, J. T.; Daran, J.-M. De Novo Production of the Flavonoid Naringenin in Engineered *Saccharomyces Cerevisiae*. *Microb. Cell Fact.* **2012**, *11* (1), No. 155.